Available online at www.sciencedirect.com

ScienceDirect

Catalysis Today 137 (2008) 493–497

CATALYSIS TODAY

www.elsevier.com/locate/cattod

Cobalt cationic sites in ferrierites: QM/MM modeling

Ewa Banach [a], Paweł Kozyra [a,*], Paweł Rejmak [b], Ewa Brocławik [b], Jerzy Datka [a]

[a] *Faculty of Chemistry, Jagiellonian University, ul. Ingardena 3, 30-060 Kraków, Poland*
[b] *Institute of Catalysis, Polish Academy of Sciences, ul. Niezapominajek 8, Kraków, Poland*

Abstract

Cobalt(II) sites in ferrierites are already well-known from their catalytic activity, their speciation and properties, however, the knowledge are far from completeness. The following paper presents the first in literature combined QM/MM study to elucidate the structure of these sites. With this end force-field parameters describing Co interactions with ionic shells in zeolite have been tested and the cell size for various Al distributions and Co positioning has been determined. Oxide-type Buckingham parameters are shown to perform better than the carbonate ones. Moreover, Co(II) ions stability in α and β sites with various Al distribution indicates at T1T1 Al substitution in β-site as that the preferred Co(II) siting. DFT results show that the quartet spin state of Co(II) is more stable than the doublet one.

Keywords: Cobalt(II) site; Ferrierite; QM/MM; NO SCR; Buckingham potential

1. Introduction

Transition metal-exchanged zeolites are active catalysts for a variety of chemical reactions [1–4]. Notable examples include the decomposition of NO and N_2O, the selective oxidation, ammoxidation, or aromatization of hydrocarbons, and the selective catalytic reduction of nitrogen oxides (NOx). Among the many factors that may control catalytic activity are the type of metal, the metal–zeolite coordination, the location of the metal in the zeolite, and the zeolite topology. Ferrierite is a particularly active zeolite for many catalytic reactions and any fundamental description of the catalytic ability of these materials must begin with the understanding of the metal active sites nature. Extraframework Co(II) sites in ferrierites are of special interest since they show enhanced activity in NOx reduction by hydrocarbons in the presence of excess oxygen, a highly desirable process in the case of lean-burn engines. Nevertheless, speciation and properties of Co(II) sites in ferrierites is still not well known. Therefore theoretical modeling has been used to elucidate the structure of the site, however, only limited number of works can be found in the literature and no final consensus has been met.

More recent DFT calculations on model cobalt–ferrierite clusters have shown that the relative arrangement of aluminum substitutions in addition to the position of the site within the zeolite determine the observed cobalt infrared, UV–vis or EXAFS signature [5,6]. Nevertheless, even if an assignment of e.g. infrared signature to extraframework site may be observed, cluster DFT calculations clearly show that the overall dependence is more complex and requires the modeling that would take into account extended framework environment of the site. A convenient method, which enables taking into account the influence of periodic lattice on catalytic center is a combined QM/MM technique. Within this approach the nearest surrounding of Co site built of several tetrahedral Si or Al units is described at accurate QM (preferably DFT) level while the periodic framework is treated by less computationally expensive approximate force-field methods. On top of that, prospective modeling of the interaction of cobalt sites with adsorbed molecules of various types additionally justifies the need of devising extended QM/MM methodology. In the present work we apply a variant of QM/MM called combined quantum mechanics/interatomic potential (QM-Pot) functions method [7]. The QM-Pot has been widely tested and shown to provide good description of copper sites in MFI or FER type zeolites and their interaction with adsorbed molecules (for example see Ref. [8–11] and references therein). However, cobalt sites in zeolites have not yet been treated by this

---

[*] Corresponding author. Tel.: +48 126632081; fax: +48 126340515.
E-mail address: kozyra@chemia.uj.edu.pl (P. Kozyra).

0920-5861/$ – see front matter © 2007 Elsevier B.V. All rights reserved.
doi:10.1016/j.cattod.2007.11.045

methodology; hence specific parameters for the interaction of Co(II) with zeolite framework are not available in the literature. Therefore the following paper addresses two problems. Firstly, the appropriate set of cobalt parameters should be selected and tested for performance with respect to properties of Co–ferrierite sites. Force-field parameters for Si, Al and O atoms are available from the precise parameterization [12]. On the other hand, parameters A_{kl} and ρ_{kl} in van der Waals Buckingham-type potential (Eq. (1)), describing short-range repulsion of Co cations with anionic shells, should be determined aiming at final QM/MM model:

$$V_{\text{short-range}} = \sum_{k,l} A_{kl} \exp(-r_{kl}\rho_{kl}^{-1}) - \sum_{k,l} C_{kl} r_{kl}^{-6} \qquad (1)$$

Assessment of Buckingham parameters requires force-field and QM/MM calculations for many types of cobalt sites in ferrierite (Co(II) positioning and Al contents) thus, in addition, our calculation results form a fairly good basis for qualitative analysis of site speciation and properties. Therefore the second goal of the paper is the assessment, description and ranking of cobalt sites in ferrierite.

2. Models and methods

The ferrierite structure (*Immm*) taken from the Cerius^2 [13] database was the basis of the models. There are four types of T-atoms. For each individual site all possible ways of substituting T-atoms with Al have been taken into account. It allowed then to analyze the influence of the distribution of aluminum on cobalt(II) stability and properties. Following Kaucky et al. [14] we have nominated three positions of cobalt cation, namely α, β and γ (Fig. 1). Al atoms were placed only in T-positions which were in the nearest neighborhood of Co(II) hence the models mimicked high Si/Al ratio. This procedure produced 9 models to be tested.

For transition metal ions dispersion term in Eq. (1) can be usually neglected [8]. Hence only Buckingham parameters A_{kl} and ρ_{kl} describing short-range Pauli repulsion were considered while aiming at final QM/MM model. As a trial testing parameters two sets available in literature have been used. The first one (BI) has been optimized for cobalt oxide: $A_{kl} = 684.9$ eV and $\rho_{kl} = 0.3327$ Å [15], while the second (BII) for carbonate: $A_{kl} = 1095.6$ eV and $\rho_{kl} = 0.2863$ Å [16]. Because Co(II) ions always appear inside QM cluster and the strongest interaction with the nearest neighbors are covered by QM calculations less accurate force-field parameters can be used for cobalt cations than for remaining lattice atoms. The main criterion of the choice of parameters for cobalt cation in zeolite was the similarity of geometry obtained with the same set of force-field parameters at MM alone and QM/MM levels, in conjunction with criterion taken by Nachtigallová et al. [9]. Parameters for other atoms (Si, Al, O, H) were adopted after Sierka and Sauer work [12].

To estimate cell parameters we performed constant pressure MM simulation for all models considered in this work and selected the cell size for the most stable one as valid for all other

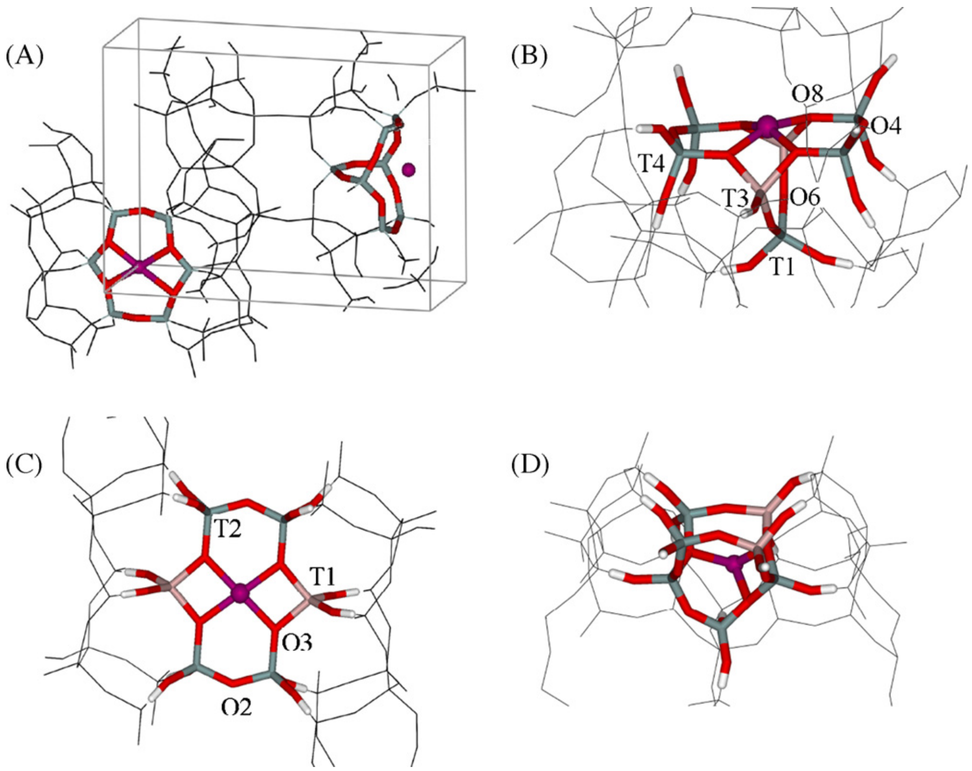

Fig. 1. (A) Positioning of α and β Co sites (relevant for further modeling) in the ferrierite, QM clusters depicted with sticks and balls; (B) α-site; (C) β-site; (D) γ-site (proposed cluster).

models. Since QM/MM calculations imply constant volume procedure, all MM optimizations were repeated with constant cell parameters within this scheme. Chosen single cell parameters are $a = 18.9954$ Å, $b = 14.1209$ Å, $c = 7.5146$ Å for BI and $a = 19.0855$ Å, $b = 14.0907$ Å, $c = 7.6064$ Å for BII, all angles equal 90.0°.

3. Computational details

All calculations have been done by the QMPOT program [17] which combines quantum chemical (QM) DFT method and molecular mechanics (MM). TURBOMOLE [18] as a part of QM-Pot constitutes a QM part while GULP [19] performs MM calculations. The gradient-corrected functional PBE [20] has been used with TZVP (*triple-ξ plus polarization*) basis set [21]. MARI-J approximation [22,23] has been applied in order to accelerate calculations. Clusters for the QM part have been terminated with hydrogen atoms. ESR experiment for Co(II)-zeolites shows quartet spin states as the most stable [24]. Additionally we have investigated doublet states, which have been suggested as possible intermediate in reactions involving Co(II) centers [6]. Sextet states have not been studied. Overall, at this stage of research, only the most stable spin states of cobalt, d^7 ion in zeolites have been considered, namely quartet – a high-spin (HS) and a doublet – a low-spin (LS) state. No symmetry constrains was imposed. Double unit cell must be applied to contain 7T (by T atoms we mean tetrahedrally coordinated Si and Al atoms) cluster for α-site clusters thus, consequently, also doubled cell have been applied for 6T β-site clusters. In all cases two Al atoms in vicinity of Co(II) ion are placed within QM clusters. All possible alumina pair distributions, satisfying Loewenstein rule [25] (Al–O–Al connectivity forbidden), for either site are investigated.

Positioning of α- and β-sites is shown in Fig. 1A. The cluster of α-site consists of 7T-atoms which are of three types: T1, T3 and T4 (Fig. 1B). There are 5 possible distributions of Al atoms in α-cluster are: T1T4, T3T3, T3T4, T4T4-*meta*, and T4T4-*para*. The β-site (Fig. 1C) it is a distorted six-member ring with two types of T atoms: T1 and T2 thus T1T1, T1T2, T2T2-*meta*, and T2T2-*para* are the allowed combinations for Al atoms. γ-Site is a cage with small rings leading inside (Fig. 1D) hence it is supposed not to be accessible for NO molecules. For this sake only the data for α- and β-sites will be presented and analyzed.

4. Results

Two criteria of Buckingham parameters assessment have been applied:

1. Conformity of geometry obtained by MM and QM/MM. Decisive factors were the distances between cobalt(II) cation and the nearest oxygen atoms (the limit of coordination radius is assumed as 2.50 Å).
2. Reproduction by MM of QM/MM energetic relations between sites of different Al distribution.

4.1. Geometric criterion

The analysis of Co(II)–O distances (Tables 1 and 2) for both sets of Buckingham parameters shows better agreement between MM and QM/MM results for the oxide-type set of parameters. We have assumed the average difference between MM and QM/MM values of Co–O distances as the geometric criterion. For the bonds shorter than 2.50 Å (depicted in bold type in Tables 1 and 2) it is +0.07 Å for oxide-type Buckingham

Table 1

Co(II)–O distances in α-site for two types of Buckingham potential (distances less than 2.50 Å are depicted bold type)

Al sites	$R_{\mathrm{Co–O}}$ (MM) (Å)		$R_{\mathrm{Co–O}}$ (QM/MM) (Å)			
	Constant volume		Doublet		Quartet	
	BI	BII	BI	BII	BI	BII
1,4						
Co–O8$_{\mathrm{Al}}$	**1.98**	**1.89**	**1.95**	**1.96**	**1.99**	**2.00**
Co–O6$_{\mathrm{Al}}$	**2.17**	**1.94**	**2.02**	**1.98**	**2.11**	**2.14**
Co–O8	**2.35**	**1.98**	**2.07**	**2.00**	**2.11**	**2.14**
Co–O8	**2.23**	**2.12**	**2.13**	**2.35**	**2.17**	**2.15**
Co–O6	3.74	3.48	4.00	4.00	3.96	3.71
Co–O8	2.47	3.42	3.59	3.45	3.51	3.34
Co–O4$_{\mathrm{Al}}$	4.34	3.22	3.43	3.29	3.56	3.37
Co–O4$_{\mathrm{Al}}$	2.69	**1.94**	3.51	**2.22**	3.56	**2.33**
3,3						
Co–O8$_{\mathrm{Al}}$	**2.04**	**1.85**	**1.97**	**1.93**	**2.02**	**2.02**
Co–O6	3.46	3.41	3.50	3.48	3.51	3.51
Co–O8$_{\mathrm{Al}}$	**2.08**	**1.91**	**1.95**	**2.00**	**2.05**	**2.06**
Co–O8$_{\mathrm{Al}}$	**2.05**	**1.84**	**1.96**	**1.93**	**2.03**	**2.02**
Co–O6	3.44	4.35	3.50	3.50	3.52	3.49
Co–O8$_{\mathrm{Al}}$	**2.08**	**1.91**	**1.94**	**2.00**	**2.05**	**2.06**
Co–O4$_{\mathrm{Al}}$	3.56	3.26	3.35	3.29	4.17	3.40
Co–O4$_{\mathrm{Al}}$	3.56	3.20	3.25	3.23	2.89	3.48
3,4						
Co–O8$_{\mathrm{Al}}$	**2.01**	**1.88**	**1.98**	**1.93**	**2.02**	**2.03**
Co–O6$_{\mathrm{Al}}$	3.07	**2.00**	3.59	**2.01**	3.57	2.15
Co–O8$_{\mathrm{Al}}$	**1.98**	**1.79**	**1.92**	**1.96**	**1.99**	**2.00**
Co–O8	**2.46**	3.54	**2.07**	3.69	**2.21**	3.58
Co–O6	3.64	3.75	3.38	4.05	3.42	3.99
Co–O8$_{\mathrm{Al}}$	**2.06**	**1.86**	**1.94**	**2.03**	**2.01**	**2.06**
Co–O4	3.69	3.40	3.33	3.59	3.55	3.68
Co–O4$_{\mathrm{Al}}$	3.35	3.30	3.13	3.29	3.31	3.37
4,4-*Meta*						
Co–O8$_{\mathrm{Al}}$	**2.09**	**1.83**	**1.98**	**1.97**	**2.02**	**2.04**
Co–O6$_{\mathrm{Al}}$	3.71	2.99	3.61	3.47	3.53	3.41
Co–O8	**2.34**	**1.88**	**2.10**	**1.98**	**2.07**	**2.07**
Co–O8	**2.43**	**2.28**	**3.23**	**2.07**	**2.19**	**2.20**
Co–O6$_{\mathrm{Al}}$	3.07	3.60	**2.14**	3.42	3.29	3.50
Co–O8$_{\mathrm{Al}}$	**2.06**	**1.81**	**1.91**	**1.91**	**2.00**	**1.98**
Co–O4	3.53	3.24	3.31	3.18	3.50	3.41
Co–O4	3.55	3.28	3.19	3.19	3.38	3.36
4,4-*Para*						
Co–O8$_{\mathrm{Al}}$	**1.99**	**1.85**	**1.97**	**2.00**	**1.99**	**2.02**
Co–O6$_{\mathrm{Al}}$	3.67	4.04	3.62	4.11	3.63	3.96
Co–O8	2.51	3.05	**2.08**	3.69	2.26	3.68
Co–O8$_{\mathrm{Al}}$	**2.01**	**1.80**	**1.92**	**1.95**	**2.01**	**2.01**
Co–O6$_{\mathrm{Al}}$	**2.17**	4.03	**2.11**	**2.00**	**2.14**	**2.08**
Co–O8	2.75	**2.03**	3.30	**1.96**	3.26	**2.15**
Co–O4	3.52	3.29	3.12	3.42	3.24	3.54
Co–O4	3.50	3.31	3.34	3.32	3.47	3.46

Table 2
Co(II)–O distances in β site for two types of Buckingham potential (distances less than 2.50 Å are depicted bold type)

Al sites	$R_{Co–O}$ (MM) (Å)		$R_{Co–O}$ (QM/MM) (Å)			
	Constant volume		Doublet		Quartet	
	BI	BII	BI	BII	BI	BII
1,1						
$Co–O3_{Al}$	**2.04**	**1.85**	**1.93**	**1.93**	**2.01**	**2.00**
$Co–O3_{Al}$	**2.01**	**1.85**	**1.96**	**1.97**	**1.99**	**2.00**
Co–O1	3.29	3.45	3.46	3.47	3.43	3.43
$Co–O3_{Al}$	**2.04**	**1.85**	**1.93**	**1.93**	**2.01**	**2.00**
$Co–O3_{Al}$	**2.01**	**1.85**	**1.96**	**1.97**	**1.99**	**2.00**
Co–O1	3.29	3.45	3.46	3.47	3.43	3.43
1,2						
$Co–O3_{Al}$	**2.00**	**1.82**	**1.95**	**1.94**	**2.02**	**2.00**
Co–O3	**2.29**	**2.12**	**2.01**	**2.02**	**2.09**	**2.11**
Co–O1	3.40	3.45	3.39	3.38	3.39	3.39
$Co–O3_{Al}$	**2.04**	**1.85**	**1.94**	**1.94**	**2.01**	**1.99**
$Co–O3_{Al}$	**1.98**	**1.82**	**1.95**	**1.95**	**1.97**	**1.98**
$Co–O1_{Al}$	2.92	3.31	3.52	3.36	3.43	3.44
2,2-*Meta*						
$Co–O3_{Al}$	**2.05**	**1.82**	**1.96**	**1.95**	**1.99**	**1.98**
$Co–O3_{Al}$	**2.03**	**1.84**	**1.91**	**1.92**	**1.98**	**2.00**
Co–O1	3.34	3.22	3.42	3.39	3.39	3.34
Co–O3	**2.46**	**2.04**	**2.08**	**2.08**	**2.13**	**2.13**
Co–O3	**2.28**	**2.10**	**2.04**	**2.05**	**2.12**	**2.15**
$Co–O1_{Al}$	**2.36**	3.30	3.39	3.40	3.35	3.37
2,2-*Para*						
$Co–O3_{Al}$	**1.95**	**1.81**	**1.88**	**1.95**	**1.91**	**1.95**
Co–O3	3.14	3.01	3.40	3.40	3.35	3.02
$Co–O1_{Al}$	**2.31**	3.79	**2.15**	4.12	**2.25**	3.91
$Co–O3_{Al}$	**1.96**	**1.88**	**1.88**	**2.08**	**1.91**	**2.07**
Co–O3	3.02	**2.08**	3.40	**1.98**	3.35	**2.11**
$Co–O1_{Al}$	**2.28**	**1.99**	**2.15**	**2.00**	**2.25**	**2.20**

parameters while for the carbonate one it is −0.16 Å. Positive value of this difference for oxide Buckingham set means that the bonds are longer for MM than for QM/MM hence the parameters for oxides underestimate short-range interaction and at the same time underestimates strength of the bonds between cobalt(II) cation and framework oxygen atoms. On the contrary Buckingham potential with BII set of parameters significantly overestimates the bonds Co–O giving shorter distances when only MM calculation is applied.

Table 3
Relative energy of the α systems (double unit cell) for different Al distribution calculated by MM and QM/MM

Al sites	*E* (MM) (kJ/mol)		*E* (QM/MM) (kJ/mol)			
	Constant volume		BI		BII	
	BI	BII	Doublet	Quartet	Doublet	Quartet
T1T4	65.75	74.52	96.88	53.37	135.47	85.94
T3T3	**0**	**0**	33.85	**0**	32.90	**0**
T3T4	14.85	13.95	45.37	9.49	77.19	44.61
T4T4-*Meta*	50.15	97.50	104.80	56.99	117.45	82.22
T4T4-*Para*	18.17	40.73	91.47	49.14	127.57	86.82

Table 4
Relative energy of the β systems (double unit cell) for different Al distribution calculated by MM and QM/MM

Al sites	*E* (MM) (kJ/mol)		*E* (QM/MM) (kJ/mol)			
	Constant volume		BI		BII	
	BI	BII	Doublet	Quartet	Doublet	Quartet
T1T1	**0**	**0**	24.00	**0**	22.56	**0**
T1T2	38.49	18.89	64.36	37.38	67.12	43.35
T2T2-*Meta*	82.76	98.94	118.04	87.46	122.09	89.25
T2T2-*Para*	49.44	49.87	101.11	71.16	157.31	105.49

4.2. *Energetic criterion*

Besides geometric matching, relative total energy can be the additional property which can help to assess results with respect to the performance of two tested Buckingham potentials. Energies obtained from MM and QM/MM calculation are set together in Tables 3 and 4 for α- and β-site, respectively. Regardless of the site, quartet is always a more stable state than a doublet. On the basis of ligand field theory such a case is realized for relatively weak interaction. Moreover, the differences between energies of HS and LS state is two times bigger for α-site than for β-site what makes the additional argument for stronger cobalt(II) interaction in β-site. This may be the reason why Co(II) ion is more stable in that type of site.

For α-site (Table 3) the order of the centers sorted out by their energy is the same for MM and QM/MM when the BI set is used. BII set of Buckingham parameters reproduces only the order of the two the most stable sites. Similarly, for β sites the agreement is better for oxide Buckingham potential (Table 4).

Having information about multiplicity and Buckingham potentials we can cut down the number of the system taken into consideration in the final discussion (HS and BI) and focus on the stability of the systems with different Al atoms distribution. The most stable systems: T3T3 for α-site and T1T1 for β-site seem to be distinguished with higher symmetry than the other systems.

5. Conclusions

The main goal of this work was the assessment of molecular mechanics parameters (Buckingham type) for QM/MM modeling of Co(II) sites in ferrierite:

(A) Force-field parameters for oxide systems give better agreement between MM and QM/MM geometry than those for carbonate.
(B) Relative energetic stabilities are also more similar within the set MM and QM/MM results if oxide parameters are used.

Therefore BI parameters may be recommended for further use. In addition, obtained results allow also for some conclusions regarding qualitative speciation of Co(II) sites in ferrierite:

1. Cobalt(II) interacts weaker with α-site than with β-site what supports the statement that it is more stable in the latter.

2. Al atoms distribution influences cobalt(II) stability. The most favorable combination of Al atoms is T3T3 for α-site and T1T1 for β-site. Judging by the energy of individual models one can conclude that the more symmetric Al atoms distribution the more stable system is.
3. Cobalt(II) cation is coordinated by four framework oxygen atoms and it is square coordinated in β-site and forms a pyramid in α-site.
4. Cobalt cation embedded in the ferrierite framework appears in high multiplicity state—it is quartet independently on the site.

These results are in full agreement with previous DFT cluster study [6]. They are indispensable initial stage for further research of interaction of cobalt sites with reagents or probe-molecules. On the other hand obtained structures of cobalt sites in ferrierite may be used to test the nature of various cobalt sites such as CoO^+, $Co(OH)^+$, etc. other than isolated cobalt ions.

Acknowledgement

This study was partly sponsored by the Polish State Committee for Scientific Research (Grant No. PZB-KBN-116/T09/2004).

References

[1] Y. Traa, B. Burger, J. Weitkamp, J. Micropor. Mesopor. Mater. 30 (1999) 3.
[2] Y. Li, J.N. Armor, Appl. Catal. B 1 (1992) L31.
[3] J.N. Armor, Catal. Today 26 (1995) 147.
[4] X. Wang, H.-Y. Chen, W.M.H. Sachtler, Appl. Catal. B 26 (2000) L227.
[5] K. Pierlot, A. Delabie, C. Ribbing, A.A. Verberckmoes, R.A. Schoonheydt, J. Phys. Chem. B 102 (1998) 10789.
[6] S.A. McMillann, L.J. Broadbelt, R.Q. Snurr, J. Phys. Chem. B 106 (2002) 10864.
[7] U. Eichler, C.M. Kölmel, J. Sauer, J. Comp. Chem. 18 (1997) 463.
[8] D. Nachtigallová, P. Nachtigall, M. Sierka, J. Sauer, Phys. Chem. Chem. Phys. 1 (1999) 2019.
[9] D. Nachtigallová, P. Nachtigall, J. Sauer, Phys. Chem. Chem. Phys. 3 (2001) 1552.
[10] M. Davidová, D. Nachtigallová, P. Nachtigall, J. Sauer, J. Phys. Chem. B 108 (2004) 13674.
[11] M. Sierka, J. Sauer, in: S. Yip (Ed.), The Handbook of Materials Modelling, Springer, Dordrecht, 2005, pp. 241–258.
[12] M. Sierka, J. Sauer, Faraday Discuss. 106 (1997) 41.
[13] Program Cerius2, Molecular Simulations Inc., Cambridge, 1993.
[14] D. Kaucky, J. Dědeček, B. Wichterlová, Micropor. Mesopor. Mater. 31 (1999) 75.
[15] G.V. Lewis, C.R.A. Catlow, J. Phys. C: Solid State Phys. 18 (1985) 1149.
[16] K.D. Fisler, J.D. Gale, R.T. Cygan, Am. Mineral. 85 (2000) 217.
[17] M. Sierka, J. Sauer, J. Chem. Phys. 112 (2000) 6983.
[18] R. Ahlrichs, M. Bär, M. Häser, H. Horn, C.M. Kölmel, Chem. Phys. Lett. 162 (1989) 165.
[19] J.D. Gale, J. Chem. Soc., Faraday Trans. 93 (1997) 629.
[20] J.P. Perdew, K. Burke, M. Ernzerhof, Phys. Rev. Lett. 77 (1996) 3865.
[21] A. Schäfer, C. Huber, R. Ahlrichs, J. Chem. Phys. 100 (1994) 5829.
[22] K. Eichkorn, O. Treutler, H. Öhm, M. Häser, R. Ahlrichs, Chem. Phys. Lett. 240 (1995) 283, 242 (1995), 652.
[23] M. Sierka, A. Hogekamp, R. Ahlrichs, J. Chem. Phys. 118 (2003) 9136.
[24] E.-M. El-Malki, D. Werst, P.E. Doan, W.M.H. Sachtler, J. Phys. Chem. B 104 (2000) 5924–5931.
[25] W. Loewenstein, Am. Mineral. 39 (1954) 92.